

# Density Profile of Dense Granular Flow down a Rough Slope

Namiko Mitarai<sup>1</sup> and Hiizu Nakanishi<sup>2</sup>

<sup>1</sup>*Frontier Research System, RIKEN, Hirosawa 2-1, Wako-shi, Saitama 351-0198, Japan.*

<sup>2</sup>*Department of Physics, Kyushu University 33, Fukuoka 812-8581, Japan.*

(Dated: January 27, 2020)

We investigate the bulk rheology of dense granular flow down a rough slope, where the density has been found constant except for the boundary layers in simulations [Silbert *et al.*, Phys. Rev. E **64**, 051302 (2001)]. It is demonstrated that both the Bagnold scaling and the framework of kinetic theory are applicable in the bulk, which allows us to extract the constitutive relations using simulation data. The detailed comparison of our data with the kinetic theory shows quantitative agreement for the normal and shear stresses, but there exists slight discrepancy in the energy dissipation, which causes rather large disagreement in the analysis of granular flow using the kinetic theory.

PACS numbers: 45.70.Mg, 45.50.-j, 47.50.+d

Flowing granular material behaves like a fluid, but comprehensive understanding of its rheology is still far from complete. In the low-density regime with large shear rate, grains interact through instantaneous collisions and are described by a hydrodynamic model based on kinetic theory of inelastic hard spheres [1]. As the system becomes denser, the independent collision assumption, that most kinetic theories depend upon, becomes questionable and the one particle distribution of grain velocity may not be characterized by a small number of parameters or temperatures. When grains are nearly closed packed, they may experience enduring contacts, in which case the system behavior resembles plastic deformation.

One of a few established laws that hold for granular rheology up to relatively dense regime is the Bagnold law [2], which states that the shear stress is proportional to the square of the strain rate. In fact, this is the only possible form for the stress in the flow of rigid grains characterized by the shear rate  $\dot{\gamma}$  and the packing fraction  $\nu$ , because  $\dot{\gamma}^{-1}$  is the only time scale involved. Simple dimensional consideration gives the Bagnold scaling for the shear stress  $S$  as

$$S = A(\nu) m \sigma^{2-d} \dot{\gamma}^2, \quad (1)$$

where  $m$  is grain mass,  $\sigma$  is grain diameter, and  $d$  is the spatial dimension, with  $A$  being a dimensionless coefficient that depends on  $\nu$ . Obviously this scaling law should have broad range of validity for a simple shear flow of cohesionless hard grains, and it should hold until either the system becomes so dense that the elasticity of particles comes into the problem or the shear banding destabilizes the uniform shear flow. In the case of gravitational flow down a slope, the shear is brought about by the gravity and the gravitational acceleration  $g$  brings another time scale into the problem, but the Bagnold law is expected to hold in denser region where the effect of gravity on particle orbits between collisions is not significant. The Bagnold scaling is actually observed in experiments [2, 3] and simulations [4] on the slope flows quite well.

Recently, Silbert *et al.* have performed large scale molecular dynamics simulations on dense slope flows [4]

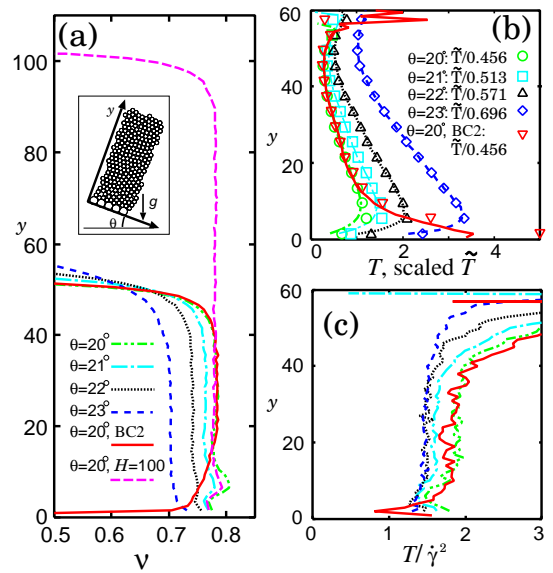


FIG. 1: (color online) The  $y$  dependences of the packing fraction  $\nu$  (a), the granular temperature  $T$  (lines) and the rotational temperature  $\bar{T}$  (marks) (b), and  $T/\dot{\gamma}^2$  (c) for various inclination angles  $\theta$ . The inset in (a) shows a schematic diagram of the system with a coordinate. For most of the data, the bottom boundary is BC1 (see text) and the total depth  $H$  is 50, but the data with BC2 and  $H = 100$  are also given for  $\theta = 20^\circ$ . In (b),  $\bar{T}$  are divided by the factors 0.456 ( $\theta = 20^\circ$ ), 0.513 ( $\theta = 21^\circ$ ), 0.571 ( $\theta = 22^\circ$ ), and 0.696 ( $\theta = 23^\circ$ ) to show  $\bar{T} \propto T$  in the bulk region.

and they found an interesting fact that the density of the flow is almost constant and independent of the depth except for the boundary layers near the bottom and the surface. This is quite intriguing if one note that the value of the constant density is not nearly closed packed density; it depends upon the inclination angle  $\theta$  but neither upon the total depth of the flow  $H$  [4] nor the roughness of the slope [5]. Somehow, the system seems to adjust its temperature variation to keep the density constant along the depth direction.

This is, however, not difficult to understand if one ex-

tends the Bagnold scaling to the pressure; under the same condition, the pressure, or the normal stress  $N$ , should have the same form

$$N = B(\nu) m \sigma^{2-d} \dot{\gamma}^2 \quad (2)$$

as  $S$  with another dimensionless coefficient  $B$ , thus the ratio of  $S/N$  depends upon the packing fraction  $\nu$ , but not on the shear rate  $\dot{\gamma}$ . In the gravitational slope flow, force balance gives  $S/N = \tan \theta$ , thus we have

$$A(\nu)/B(\nu) = \tan \theta, \quad (3)$$

which means the packing fraction is determined by the inclination  $\theta$  but does not depend upon the depth  $H$ . This argument suggests the existence of the bulk region with the constant density in the gravitational flow is very general and independent of detailed properties of grains.

In order to determine how the packing fraction  $\nu$  depends on  $\theta$ , we need a theory that gives constitutive relations. This has been done by Louge [6] using a kinetic theory for inelastic hard spheres [7]. It is disappointing, however, to find that the kinetic theory fails to give correct density profiles; two branches of solution for  $\nu$  were found, but one gives too small value for  $\nu$  and the other gives opposite  $\theta$  dependence of  $\nu$  to the one observed in simulations, implying the branch corresponds to a dynamically unstable one. This is a little puzzling situation because the kinetic theory has been shown to hold in the case of sheared flow of similar density regime [8].

In this paper, we perform detailed analysis of our simulations on the bulk region of two-dimensional gravitational flow, assuming the framework of kinetic theory. In contrast to previous works where the overall profiles from hydrodynamic models were discussed [9], we examine each constitutive relations separately using data in the bulk to avoid the uncertainty in a boundary condition for hydrodynamic equations.

First, we show how the bulk behavior is understood within the framework of kinetic theory. In the granular kinetic theory, the kinetic temperature  $T \equiv m <(\mathbf{c} - \mathbf{v})^2> / d$  is treated as a separate variable, which introduces an additional time scale. Here,  $\mathbf{c}$  is particle velocity,  $<\dots>$  represents average over microscopic scales, and  $\mathbf{v} = <\mathbf{c}>$ . The shear stress is given by the momentum flux, which is  $m \ell(\nu) \dot{\gamma} n \sqrt{T/m}$  from the elementary transport theory, where  $n$  is the number density and  $\ell(\nu)$  represents the mean free path. This gives

$$S = f_2(\nu) m^{1/2} \sigma^{1-d} T^{1/2} \dot{\gamma}, \quad (4)$$

where  $f_2(\nu)$  is a dimensionless function of  $\nu$  and other material parameters such as a restitution coefficient. Similarly we have for the normal stress  $N$ , the energy dissipation  $\Gamma$ , and the heat flux  $q$

$$N = f_1(\nu) \sigma^{-d} T, \quad (5)$$

$$\Gamma = f_3(\nu) m^{-1/2} \sigma^{-d-1} T^{3/2}, \quad (6)$$

$$q = -f_4(\nu) m^{-1/2} \sigma^{1-d} T^{1/2} \partial_y T. \quad (7)$$

The forms (4) to (7) represent quite general framework in kinetic theory, although functional forms  $f_i(\nu)$  vary depending upon level of approximation.

These expressions should be compatible with the Bagnold scaling when the only relevant time scale is  $\dot{\gamma}^{-1}$ . Equation (4) of  $S$  indicates that  $T \propto \dot{\gamma}^2$  in order that the Bagnold scaling (1) should hold. In the kinetic theory,  $T$  is determined by the energy balance equation

$$-\partial_y q + S \dot{\gamma} - \Gamma = 0 \quad (8)$$

in the steady flow. When the divergence of heat flux  $-\partial_y q$  is zero as in the case of the uniform shear flow due to the symmetry in the  $y$ -direction,  $T$  is determined by the local balance between the viscous heating  $S \dot{\gamma}$  and the energy loss  $\Gamma$ ; then the time scale that determine  $T$  is the shear rate only.  $S \dot{\gamma} = \Gamma$  with Eqs. (4) and (6) gives

$$T = [f_2(\nu)/f_3(\nu)] m \sigma^2 \dot{\gamma}^2, \quad (9)$$

thus the Bagnold law holds. In the slope flow, the divergence of heat flux is not necessarily zero, but it turns out to be small compared with the other terms. Therefore, from Eqs. (4), (5), (9), and  $S/N = \tan \theta$ , we have

$$\tan \theta = \sqrt{f_2(\nu) f_3(\nu)} / f_1(\nu), \quad (10)$$

which gives  $\nu$  as a function of  $\theta$  if we know  $f_i(\nu)$ .

In the following, the above analysis is examined in detail in comparison with the data of our two-dimensional simulations on the soft sphere model with disk mass  $m$ , diameter  $\sigma$ , and moment of inertia  $I = m \sigma^2 / 10$  as in Ref. [4]. The particles are taken to be hard enough so that the flow behavior does not change in the hard sphere limit [10]. The linear spring-dashpot model and the Coulomb friction with the coefficient  $\mu = 0.5$  are employed, and the periodic boundary condition is imposed along the flow direction. The bottom boundary is made rough by attaching disks of diameter  $2\sigma$ , which we refer to as BC1: See Ref. [4] for detailed description of the simulation model [11]. We confirmed that our data agree with theirs in the bulk, though our slope length ( $20\sigma$ ) is shorter than theirs ( $100\sigma$ ). We show only the data for  $\theta \geq 20^\circ$  with  $H = 50$ , which is well above the stopping angle  $\theta_{\text{stop}}$  ( $\theta_{\text{stop}} \approx 18^\circ$  [4]); the boundary effects become significant for  $\theta$  closer to  $\theta_{\text{stop}}$  [5]. The boundary effects are examined by simulating with a slope covered with disks of diameter  $\sigma$  (BC2).

To compare our data with the kinetic theory, we use the normal restitution coefficient  $e_p = 0.92$  and the tangential restitution coefficient  $\beta = 1$ , although the tangential restitution coefficient in the simulation is not constant because of sliding collisions with the Coulomb friction [12]. The Coulomb friction is important in simulation, but no kinetic theories have been worked out yet with it in two-dimension [13].

Figure 1 shows the  $y$ -dependence of  $\nu$  (a),  $T$  (b), and  $T/\dot{\gamma}^2$  (c) for various inclination angles  $\theta$ ; most of the data are for the system with the depth  $H = 50$  and BC1,

TABLE I: The constitutive relations from kinetic theory in Ref. [14], with parameters  $\kappa = 4I/(m\sigma^2)$ ,  $a = \kappa(1+\beta)/[2(1+\kappa)]$ ,  $r = (1+e_p)/2$ , and  $C = \left[-(1-\tilde{T}/T)a^2 + (5-8r)a + 2(5-3r)\right]/2$ .  $g_0(\nu)$  is the radial distribution function.

$f_1$	$(4/\pi)\nu(1+2r\nu g_0(\nu))$
$f_2$	$(1/Cg_0(\nu)\sqrt{\pi})(1+\nu g_0(\nu)(r+a))\left[1+\nu g_0(\nu)[(3r-2)r+2ar-a^2(1+\tilde{T}/\kappa T)]\right] + (4\nu^2 g_0(\nu)r/\pi^{3/2})(1+a/2r)$
$f_3$	$(4\nu^2 g_0(\nu)r/\pi^{3/2})\left[8(1-e_p)+4\kappa(1+\beta)(1+e_p)^{-1}(1+\kappa)^{-2}[2+\kappa(1-\beta)-(1+\beta)\tilde{T}/T]\right]$

but the data for BC2 and those for  $H = 100$  are also shown for  $\theta = 20^\circ$  to see the boundary condition and the depth dependence. The data are given in the unit system where the length  $\sigma$ , the mass  $m$ , and the time  $\sqrt{\sigma/g}$  are unities. One can see that the packing fraction in the bulk does not depend on the depth, and the effects of the boundary condition are confined within the boundary layer and the bulk properties are independent of it. The profiles of  $T/\dot{\gamma}^2$  in Fig. 1(c) shows that Eq. (9) holds approximately in the bulk. We have also confirmed that  $\partial_y q$  is much smaller than  $S\dot{\gamma}$  and  $\Gamma$  in the bulk, which is consistent with our argument to derive Eq. (9).

We compare our data with the constitutive relations derived by Jenkins and Richman [14] for two-dimensional inelastic hard disks. The functions  $f_1(\nu)$ ,  $f_2(\nu)$ , and  $f_3(\nu)$  in the steady flow are given in Table I. We adopt the radial distribution function  $g_0(\nu)$  from Ref. [15]

$$g_0(\nu) = g_c(\nu) + \frac{g_f(\nu) - g_c(\nu)}{1 + \exp(-(\nu - \nu_0)/m_0)}, \quad (11)$$

where  $g_c(\nu) = (1 - 7\nu/16)(1 - \nu)^{-2}$  and  $g_f(\nu) = [(1 + e_p)\nu(\sqrt{\nu_c/\nu} - 1)]^{-1}$  with  $\nu_c = 0.82$ ,  $\nu_0 = 0.7006$ , and  $m_0 = 0.0111$ .

In  $f_2(\nu)$  and  $f_3(\nu)$ , the rotational temperature  $\tilde{T} \equiv I <(\omega - \omega)^2>$  appears as  $\tilde{T}/T$ , where  $w$  is the particle angular velocity and  $\omega = <\omega>$ : In the kinetic theory,  $\omega$  is simply assumed to be  $(\nabla \times \mathbf{v})_z/2$  [14], which holds except for the region near the bottom boundary [16].  $\tilde{T}/T$  becomes constant in the kinetic theory [14]; the value should be 1 for our parameters, but is not in the simulations. This should be mainly due to the Coulomb friction, which has strong effects on particle rotations. In Fig. 1(b),  $\tilde{T}$ 's are plotted by marks along with  $T$ 's (lines):  $\tilde{T}$ 's are divided by factors with which they coincide with  $T$ 's best. One can see  $\tilde{T}$ 's fits with  $T$  in the bulk region with the factor, but the ratio depends on  $\theta$  and around 0.5. In the following, we try both 1 and the values obtained from the simulations for  $\tilde{T}/T$  in  $f_2(\nu)$  and  $f_3(\nu)$ .

First, we examine Eqs. (4) and (5). Figures 2(a) and (b) show  $N/T$  and  $S/(\dot{\gamma}\sqrt{T})$  from the simulation data, respectively, against  $\nu$  by marks. The data from the bottom layers ( $y \leq 10$ ) are distinguished by filled marks because they follow different trend. The data outside the bottom layers ( $y > 10$ , open marks) for various  $\theta$  collapse onto a single line. This clearly shows that the expressions (4) and (5) in the kinetic theory are valid

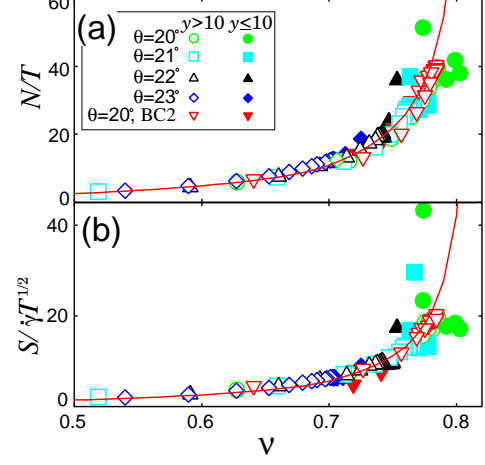


FIG. 2: (color online)  $N/T$  (a) and  $S/(\sqrt{T}\dot{\gamma})$  (b) vs.  $\nu$  for various  $\theta$ . The open and filled marks represent the data outside and within the bottom boundary, respectively. The lines show  $f_1(\nu)$  (a) and  $f_2(\nu)$  (b).

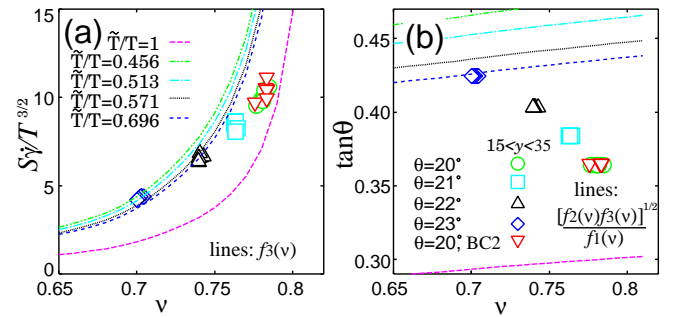


FIG. 3: (color online)  $S\dot{\gamma}/T^{3/2}$  vs.  $\nu$  (marks) with  $f_3(\nu)$  (lines) (a), and  $\tan\theta$  vs. the bulk density (marks) with  $\sqrt{f_2(\nu)f_3(\nu)}/f_1(\nu)$  (lines) (b) for various  $\theta$ . The lines represent the plots with various values of  $\tilde{T}/T$ .

outside the bottom layers. The data from the bottom layers show some scatter and different tendency between BC1 and BC2.

$f_1(\nu)$  and  $f_2(\nu)$  in Table I with  $\tilde{T}/T = 1$  are shown by the solid lines in Figs. 2(a) and (b), respectively, which agree with the data.  $f_2(\nu)$  depends on  $\tilde{T}/T$  only weakly and the difference turned out to be negligibly small in the range  $0.5 \lesssim \tilde{T}/T \lesssim 1$ .

Now, we examine  $f_3(\nu)$  in Eq. (6). In Fig. 3(a), we plot

$S\dot{\gamma}/T^{3/2}$  against  $\nu$  from the simulation data; this quantity should become  $f_3(\nu)$  from Eqs. (9) and (4). Only the data from the bulk ( $15 < y < 35$ ) are plotted because Eq. (9) is valid only in the bulk as we have already seen in Fig. 1(c). The lines show  $f_3(\nu)$  from kinetic theory with various  $\tilde{T}/T$ ; one can see  $f_3(\nu)$  depends on  $\tilde{T}/T$ . The data agrees reasonably well with  $f_3(\nu)$  when  $\tilde{T}/T \sim 0.5$ , but note that the singularity at  $\nu = \nu_c$  seems to be weaker in the simulation data than in  $f_3(\nu)$ .

This difference in  $f_3(\nu)$  is significant when we see them in resulting bulk density. In Fig. 3(b), the relation between the bulk density  $\nu$  and the inclination angle  $\theta$  is shown for the simulation data and for the kinetic theory; for the latter, we plot  $\sqrt{f_2(\nu)f_3(\nu)}/f_1(\nu)$ , which should give  $\tan \theta$  from Eq. (10). The bulk density decreases as  $\theta$  increases in the simulation, but  $\sqrt{f_2(\nu)f_3(\nu)}/f_1(\nu)$  shows opposite tendency; the density increases as  $\theta$  increases. This discrepancy comes mainly from the discrepancy in  $f_3(\nu)$ , more specifically from the fact that the data shows a weaker divergence in  $f_3(\nu)$ , while the kinetic theory assumes the same singularity in all of  $f_1(\nu)$ ,  $f_2(\nu)$ , and  $f_3(\nu)$  near the random closed packing.

Some parts of the discrepancy might originate from the Coulomb friction, which is included in the simulation and should have some effects on energy dissipation, but not taken into account in the existing two-dimensional theories. The comparison with the existing three-dimensional theory [7], however, suggests that the way it changes  $f_3(\nu)$  is just to modify the coefficient of  $\nu^2 g_0(\nu)$  as long as the level of approximation remains the same, which is not enough to make the singularity in  $f_3(\nu)$  weaker.

It is a bit puzzling to find a clear deviation from the kinetic theory in the energy dissipation while the stresses agree quite well. A possible origin of this is the velocity correlation induced by the inelasticity, which could violate the molecular chaos assumption in the kinetic theory; the decrease of the relative velocity tends to reduce the

energy loss per collision. This effect has been noticed in some granular gas simulations [17], and it is likely that the velocity correlation has more effects on the energy loss rate than on the stresses. Careful analysis of the velocity correlation is awaited.

Before concluding, let us make some comments on Pouliquen's flow rule [3]: The flow velocity at the surface is scaled as  $u(H)/\sqrt{gH} = bH/H_{\text{stop}}(\theta)$  with  $H_{\text{stop}}(\theta)$  being the depth of the flow below which flow stops for a given inclination angle  $\theta$ , and  $b$  is a numerical constant abound 0.136. Ertaş and Halsey [18] argued that the appearance of  $H_{\text{stop}}(\theta)$  in the expression of flow velocity for the depth  $H$ , which can be much larger than  $H_{\text{stop}}(\theta)$ , implies that the rheology of the dense gravitational flow is not local, and proposed the eddy mechanism. If the flow is controlled by a non-local mechanism, there is no way that the kinetic theory holds. The Pouliquen flow rule, however, does not necessarily means a non-local mechanism but it simply means the stopping depth is determined by some aspects of flowing rheology. We do not know yet how it is determined, but the present results suggest that the kinetic theory may well be a good starting point to describe the flow.

In summary, by careful analysis of simulation data, we have demonstrated that the rheology of gravitational granular flow can be described within the framework of kinetic theory. Especially, the constitutive relations by the kinetic theory have been shown to agree quantitatively with the simulations, but there is a slight discrepancy in the energy dissipation. Due to this discrepancy, the kinetic theory fails to give a correct description of the density profile of the granular flow down a slope.

N.M. thanks M. Y. Louge for insightful discussions. N.M. is supported by the Special Postdoctoral Researcher Program in RIKEN. H.N. is supported by a Grant-in-Aid for scientific research (C) 16540344 from JSPS.

---

[1] J. T. Jenkins and S. B. Savage, *J. Fluid Mech.* **130**, 187 (1983); C. S. Campbell, *Annu. Rev. Fluid Mech.* **22**, 57 (1990).

[2] R. A. Bagnold, *Proc. R. Soc. London A* **225**, 49 (1954).

[3] O. Pouliquen, *Phys. Fluids* **11**, 542 (1999).

[4] L. E. Silbert *et al.*, *Phys. Rev. E* **64**, 051302 (2002).

[5] L. E. Silbert, G. S. Grest, S. J. Plimpton, and D. Levine, *Phys. Fluids* **14**, 2637 (2002).

[6] M. Y. Louge, *Phys. Rev. E* **67**, 061303 (2003); in Proceedings of International Conference on Multiphase Flow, Yokohama, 2004, paper no. K13.

[7] J. T. Jenkins and C. Zhang, *Phys. Fluids* **14**, 1228 (2002).

[8] H. Xu, M. Louge, and A. Reeves, *Continuum Mech. Thermodyn.* **15**, 321 (2003).

[9] E. Azanza, R. Chevoir, and P. Moucheront, *J. Fluid Mech.* **400**, 199 (1999); L. Bocquet, J. Errami, and T. C. Lubensky, *Phys. Rev. Lett.* **89**, 184301 (2002).

[10] N. Mitarai and H. Nakanishi, *Phys. Rev. E* **67**, 021301 (2003).

[11] Our model corresponds to the model L2 in Ref. [4].

[12] S. Foerster, M. Y. Louge, H. Chang, and H. Allia, *Phys. Fluids* **6**, 1108 (1994).

[13] Another problem about the two-dimensional system might be its strong tendency of crystallization. In the shear flow of the present parameter region, however, the local structure is changing in time and the system does not develop a long range order.

[14] J. T. Jenkins and M. W. Richman, *Phys. Fluids* **28** (1985) 3485.

[15] D. Volfson, L.S. Tsimring, and I. S. Aranson, *Phys. Rev. E* **68**, (2003) 021301.

[16] N. Mitarai, H. Hayakawa, and H. Nakanishi, *Phys. Rev. Lett.* **88**, 174301 (2002).

[17] C. Bizon, M. D. Shattuck, J. B. Swift, and H. L. Swinney, *Phys. Rev. E* **60**, 4340 (1999); R. Kawahara and H. Nakanishi, *J. Phys. Soc. Jpn.* **73**, 68 (2004).

[18] D. Ertaş and T. C. Halsey, *Europhys. Lett.* **60**, 931 (2002).